Received: 2 February 2021 | Accepted: 23 June 2021

DOI: 10.1111/cpf.12721

ORIGINAL ARTICLE

Clinical Physiology and Functional Imaging

Physiological significance of pre- and post-ejection left ventricular tissue velocities and relations to mitral and aortic valve closures

Asbjørn Støylen[1,2] | **Annichen Søyland Daae**[1,2]

[1]Department of Circulation and Medical Imaging, Norwegian University of Science and Technology, Trondheim, Norway

[2]Department of Cardiology, St. Olav Hospital/Trondheim University Hospital, Trondheim, Norway

Correspondence
Asbjørn Støylen, Department of Circulation and Imaging, Dr. med. NTNU, Norwegian University of Science and Technology, PO Box 8905, Trondheim 7491, Norway.
Email: asbjorn.stoylen@ntnu.no

Funding information
Helse Midt-Norge, Grant/Award Number: 216/29014

Abstract

Background: Tissue Doppler shows short duration velocity spikes during pre- and post-ejection (protodiastole). They have been assumed to be isovolumic contraction and relaxation movements, but this is not in accordance with newer studies.

Methods: We examined 22 healthy volunteers. Valve closures and openings were determined from spectral Doppler from LVOT and mitral inflow and transferred to colour tissue Doppler recordings for comparison with tissue velocities, colour M-mode and strain rate (SR).

Results: Pre-ejection positive velocity spikes were simultaneous in both walls, starting ca. 24.8 ± 10.1 ms after start QRS, duration 51.5 ± 10.8 ms, ending 10.2 ± 11.5 ms after mitral valve closure (MVC) ($p < 0.001$). There were corresponding colour tracings and negative strain rate. Protodiastolic lengthening was predominant in the septum. Negative velocity spikes had a duration of 35.5 ± 10.7 ms, ending 9.5 ± 14.7 ms after aortic valve closure (AVC, $p < 0.001$) in septum. During isovolumic relaxation, strain rate showed apical lengthening (Peak SR−0.72 ± 0.50 s^{-1}) and basal shortening (Peak SR 0.44 ± 0.63 s^{-1}).

Conclusion: Electromechanical activation of the LV is simultaneous in septum and lateral wall, occurs before MVC, is terminated by MVC itself and is thus not isovolumic. Protodiastole is a short event of lengthening, predominantly in the septum. It may be the mechanism for valve closure and ends by AVC itself. Isovolumic relaxation occurs after this velocity spike, and is characterized by elongation of the apex, shortening of the base, thus showing a volume shift from base towards apex.

KEYWORDS

electromechanical activation, isovolumic relaxation, protodiastole, time intervals, tissue Doppler

1 | INTRODUCTION

With tissue Doppler imaging (TDI), short duration velocity spikes are visible at pre- and post-ejection both in spectral and colour TDI (Figure 1). The positive pre-ejection spike has been believed to belong to isovolumic contraction (IVC) (Derumeaux, et al., 1998; Edvardsen, et al., 2002; Lind, et al., 2006; Lyseggen, et al., 2005; Vogel, et al., 2002), that is, after mitral valve closure (MVC). However, initial pressure increase, and ventricular–atrial pressure crossover, occurs up to 40 ms before MVC (Dean, 1916; Hirschfeld, et al., 1976; Laniado, et al., 1973; Tsakiris, et al., 1978; Wiggers, 1921), indicating active contraction starting before MVC. With ultra-high frame rate TDI (UHFR-TDI) of >1000 frames per second (FPS), we demonstrated directly that the pre-ejection spike occurred before MVC (Brekke, et al., 2014).

The negative post-ejection velocity is seen both with TDI and colour M-mode (CAMM), and as elongation with strain rate imaging (SRI). This has been assumed to be isovolumic relaxation (IVR), starting with aortic valve closure (AVC) (Derumeaux, et al., 1998; Edvardsen, et al., 2002; Kjaergaard, et al., 2005; Lind, et al., 2006; Van de Veire, et al., 2008; Voigt, et al., 2003). With high frame rate SRI and phonocardiography, we observed that the initial elongation in mid-septum at end ejection occurred before onset of the second heart sound (A2), that is, before AVC (Slørdahl, et al., 2001). Later, both with phono (Aase, et al., 2006) and with high frame rate (>250 FPS) of the aortic valve (Aase, et al., 2008), we demonstrated AVC at the end of the negative post-ejection velocity. The aortic pressure curve shows a short, rapid decline in pressure, ending with a minimum at the dicrotic notch (Spencer & Greiss, 1962; Wiggers, 1921). The dicrotic notch itself coincides exactly with the AVC as shown with phonocardiography, M-mode and Doppler (Hatle, 1981; Hirschfeld, et al., 1977). In animal experiments, Remme et al., (2008) showed that the dicrotic notch coincided with the end of the post-ejection spike.

True isovolumic relaxation period (IVR), starting with AVC, is thus after the end of the post-ejection spike. During IVR, intraventricular flow from base to apex has been demonstrated (Sasson, et al., 1987), which was demonstrated to occur after AVC, and thus, not concomitant with the post-ejection TDI spike. The finding of intraventricular apical flow is consistent with a pressure gradient in the same direction (Nikolic et al., 1995), indicating a volume shift from base to apex during IVR.

The aim of this study was to elucidate the physiology of the pre- and post-ejection deformations in relation to the valve closures and the IVR.

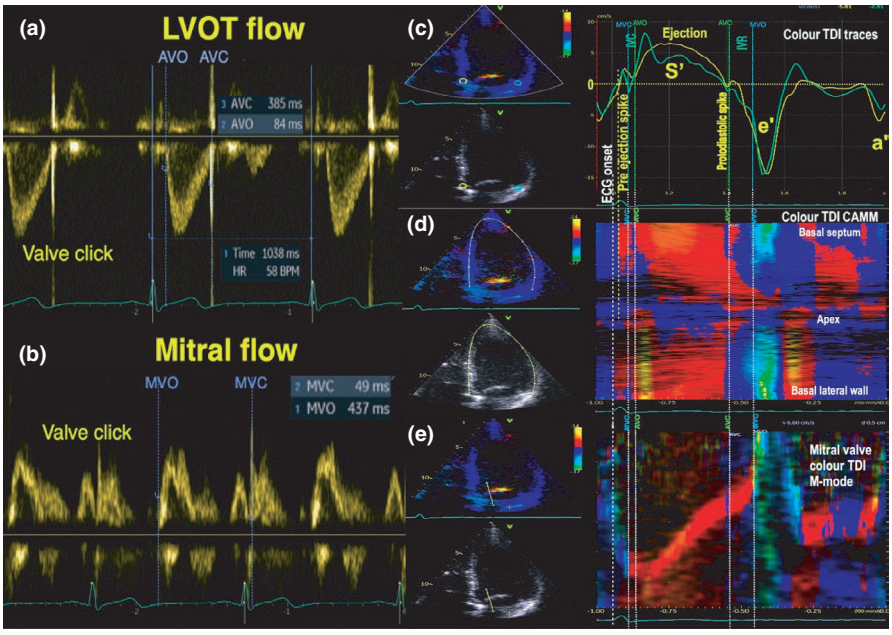

FIGURE 1 Spectral Doppler, colour tissue Doppler tracings, colour M-mode of walls and the anterior mitral leaflet from the same individual. (a) Left ventricular outflow (LVOT). Aortic valve opening (AVO) is seen by start of flow, closure (AVC) by the valve click. (b) Mitral flow, mitral valve opening (MVO) by start of early flow, closure (MVC) by the valve click. Timings are relative to the ECG marker. Valve openings and closures are automatically transferred from spectral Doppler to the TDI analysis window. (c) Numerical colour tissue Doppler traces from the mitral annulus, showing pre-ejection spike, ejection (S′), post-ejection spike and early (e′) and late (a′) velocities. (d) Curved colour M-mode (CAMM) from the same cycle, drawn from the basal septum through the apex to the base of the lateral wall. Positive velocities are shown in red, negative velocities in blue. Thus, colour transitions occur where the tracings cross the zero line. (e) A straight line M-mode through the anterior mitral leaflet. During diastolic filling phases, the mitral leaflets have rapid independent motion from the base of the ventricle seen by aliased colour, during ejection the valve mainly follows the motion of the ventricular base

2 | METHODS

2.1 | Study subjects

Twenty-two healthy volunteers (16 male, 6 female) were included in the study. One subject was excluded because of too great difference between heart rate (HR) in tissue Doppler and Doppler recordings, leaving 15 male and 6 female subjects. The study was approved by the regional ethics committee, and written informed consent was obtained. Basic characteristics of the participants are given in Table 1.

2.2 | Echocardiography

The patients were examined by an experienced cardiologist in the left lateral supine position, with an M5Sc probe on a GE E95 ultrasound scanner (GE Vingmed).

Two-dimensional apical four-chamber and long-axis B-mode images, apical four-chamber colour tissue Doppler (cTDI), as well as pulsed and continuous Doppler flow recordings were acquired. B-mode frame rate was 77 FPS, tissue Doppler frame rate was 133 FPS with background B-mode frame rate of 33 FPS.

Echo acquisitions were analysed offline in a designated analysis software (EchoPAC BT 203; GE Vingmed). Ejection fraction (EF) and end diastolic volume (EDV) were measured by the automated algorithm in echoPac, but by modified Simpson's method in four-chamber and apical long-axis B-mode views. Mitral annular plane systolic excursion was measured by reconstructed longitudinal M-mode through the mitral annulus as the average of inferoseptal and anterolateral points in four-chamber view, mitral annular velocities by spectral tissue Doppler from the same two points. Basic echocardiographic measures are likewise given in Table 1, as they are population characteristics rather than study results.

Mitral and aortic valve opening (MVO and AVO) and closure (MVC and AVC) were timed by Doppler flow; openings by start of flow, closures by valve clicks (Figure 1a,b), blinded to the cTDI recordings. HR was likewise measured directly in the same Doppler recordings by the RR interval. Systolic time intervals from spectral Doppler were calculated and are given in Table 1. Valve openings and closures were automatically transferred to the cTDI analysis package by EchoPac. HR was also measured by direct measurement of RR interval in the cTDI recordings for comparison with the spectral Doppler.

Details of TDI measurements are given in Figure 1. Mitral annular velocity curves by cTDI were analysed in the septum and lateral wall of the four-chamber view (Figure 1c), including time from start of QRS to start of pre-ejection spike, duration and peak of the pre-ejection spike and time from MVC marker to the end of the pre-ejection spike. In post-ejection, we measured duration and nadir of the negative spike and time from AVC to the end of the post-ejection spike. End of pre- and post-ejection spikes was marked either by the crossing of the velocity curve and the zero line, or by the nadir/peak of the curve where it did not cross zero. Curved anatomic M-mode (CAMM) through the whole of the septum and lateral wall was drawn for assessment of the feasibility of assessing the phases from colour display (Figure 1d). Finally, a straight line colour M-mode was placed through the septal portion of the anterior mitral leaflet in order to ascertain the presence and timing of the phases by velocity colour imaging of the mitral valve (Figure 1e).

Strain rate (Figure 2) was measured with a strain length of 20 mm and displayed in CAMM (Figure 2a) and in strain rate traces (Figure 2B,C). Peak pre- and post-ejection strain rate was measured in a region of interest of 6 × 40 mm for representativity of the whole wall (Figure 2b), while peak strain rate in IVR was measured separately in basis and apex in regions of interest of 6 × 24 mm for comparison of base and apex (Figure 2c). Default smoothing was applied; 30 ms average smoothing for velocities and 40 ms Gaussian smoothing for strain rate. Temporal resolution in TDI analysis was 10 ms.

2.3 | Statistics

Statistics were done in SPSS V.25 (IBM). Normality was tested using the Shapiro–Wilk test. Values are given by mean and standard deviations, as they were near normally distributed.

Significance of time difference between event marker by valve closure and TDI marker was by one sample *t*-test, differences in velocity, duration and strain rate between walls and levels were by paired sample *t*-test.

3 | RESULTS

Time intervals by Doppler flow measurements are given in Table 1. In short, mean IVC was 34.8 ms, left ventricular ejection time (LVET) 304.6 ms and IVR 57.1 ms. Mean HR in the Doppler recordings was 64.1 beats per minute (SD 9.1), and in colour TDI 65.8 (9.1). The difference was significant ($p < 0.001$) by pairwise *t*-test, mean difference was 1.67, with an SD of the difference of 3.6.

Timings by TDI are given in Table 2.

3.1 | Pre ejection

A pre-ejection positive velocity spike was present in both walls in all subjects before MVC, starting on the average 24.8 ms after start of QRS. Mean duration of the pre-ejection spike was 51.5 ms, peak amplitude was 3.37 cm/s and the end of the pre-ejection spike was on the average 10.2 ms after MVC ($p < 0.001$). None of these measurements differed between septum and the lateral wall. AVO was on the average 2.8 ms before the rapid upstroke of main systolic tissue velocity ($p < 0.001$), and not significantly different between walls.

TABLE 1 Basic and echocardiographic characteristics of the study subjects

Age (years)	33 (25–66)
Height (cm)	175.2 (5.6)
Weight (kg)	72.9 (10.1)
Systolic BP (mmHg)	128.1 (16.1)
Diastolic BP (mmHg)	82.3 (11.4)
EDV (ml)	120.4 (18.8)
EF (%)	55 (8)
MAPSE (mm)	15.2 (2.0)
Mitral flow E (cm/s)	84.2 (19.8)
E/A ratio	1.60 (0.46)
TDI S′ (cm/s)	10.0 (1.4)
TDI e′ (cm/s)	14.1 (3.6)
TDI a′ (cm/s)	8.0 (1.7)
HR in spectral Doppler (BPM)	64.1 (9.1)
Doppler IVC (ms)	34.8 (9.9)
Doppler LVET (ms)	304.6 (22.8)
Doppler IVR (ms)	57.1 (22.8)

Note: Values are mean with standard deviations in parentheses, except age, which is given by median and range.

Abbreviations: A, mitral flow late filling peak velocity; a′, Peak late diastolic mitral annular plane velocity; BP, blood pressure; E, mitral flow early filling peak velocity; e′, Peak early diastolic mitral annular plane velocity; EDV, end diastolic volume; EF, ejection fraction; IVC, isovolumic contraction time; IVR, isovolumic relaxation time; LVET, left ventricular ejection time; MAPSE, Mitral annular plane systolic excursion; S′, Peak systolic mitral annular plane velocity; TDI, Spectral tissue Doppler imaging.

By CAMM, positive velocities before MVC were visible in all subjects, but end of positive velocities was visible by a short blue event during IVC in the septum of eight subjects, lateral wall in 14 subjects and not at all in three subjects. Average time distance between the blue-to-red transition and the AVO marker was 0.0 ms. This can be seen in Figure 1c. MVC was visible in all subjects by the end of downward leaflet motion. The pre-ejection positive velocities were not visible. A short negative event could be seen in 10 subjects, ending with blue-to-red transition, coinciding with AVO with no time difference.

This event was only visible by mitral leaflet M-mode, but when visible coincided likewise with AVO marker with no time difference.

Pre-ejection shortening was visible in both walls, in all subjects by both colour SRI and quantitative SRI (Figure 2) before MVC, although the noisiness of strain rate gives less exact timing both in colour M-mode and traces. Peak pre-ejection strain rate was −0.72 s^{-1}, with no significant difference between walls. The interval between MVC and AVO as defined by spectral Doppler is isovolumic contraction (IVC). Including the pre-ejection spike in IVC would about double the IVC duration.

3.2 | Post-ejection lengthening

At end ejection, a short duration negative velocity spike was visible before AVC, in both septum and lateral wall of all subjects. One subject had no discernible spike, but still negative velocity before AVC. Mean post-ejection peak velocity was −1.89 cm/s, with no significant difference between walls, although this was when absolute negative velocities were taken into account. From Figure 1C, it is evident that this may not be representative for the height of the spike itself, which is lower in the lateral wall, despite a more negative value. Mean duration of the spike was 38.0 ms, again with no difference between walls. The AVC marker occurred on the mean 9.5 ms before the end of the septal spike ($p < 0.001$) and 23 ms before the end of the lateral spike (difference between walls $p < 0.001$).

In CAMM, negative velocities before AVC were visible in the septum of all subjects, and in the lateral wall only in 11. The end of this negative velocity was only visible by blue-to-red transition in 12 subjects in the septum, six subjects in the lateral wall. In the septum, the duration was 29.1 ms, significantly ($p < 0.005$) lower than by velocity traces. AVC was seen 3.3 ms before the end of the blue colour (NS). In the mitral leaflet, negative velocities were visible in 19 subjects, but the end by blue-to-red transition in only 10. In these 10, duration of the post-ejection phase was 21.4 ms, and the end was 2.5 MS before AVC (NS).

Post-ejection lengthening before AVC was visible by SRI CAMM in the septum of all subjects, but only in 13 of the lateral walls. The elongation by colour was most pronounced in the mid-septum. This is shown in Figure 2.

3.3 | Isovolumic relaxation

During IVR, between AVC and MVO markers, a basal shortening and apical elongation were visible in both walls in all subjects with mean negative strain (shortening) of −0.71 s^{-1} in the base and mean positive strain (elongation) of 0.44 in the apex as seen in Table 2.

4 | DISCUSSION

The main findings of this study are:

- Initial LV shortening is seen as a positive velocity spike in both walls by TDI, starting about 25 ms after onset of ECG, and before MVC, ending close to MVC. It is also visible as a separate shortening event by SRI. It is not part of the IVC.
- Initial post-ejection LV elongation is seen by a negative velocity spike in TDI, elongation by SRI, predominantly in the septum, after ejection. It ends with AVC and is not part of the IVR.
- During IVR, there is simultaneous elongation of the LV apex, and shortening of the base.

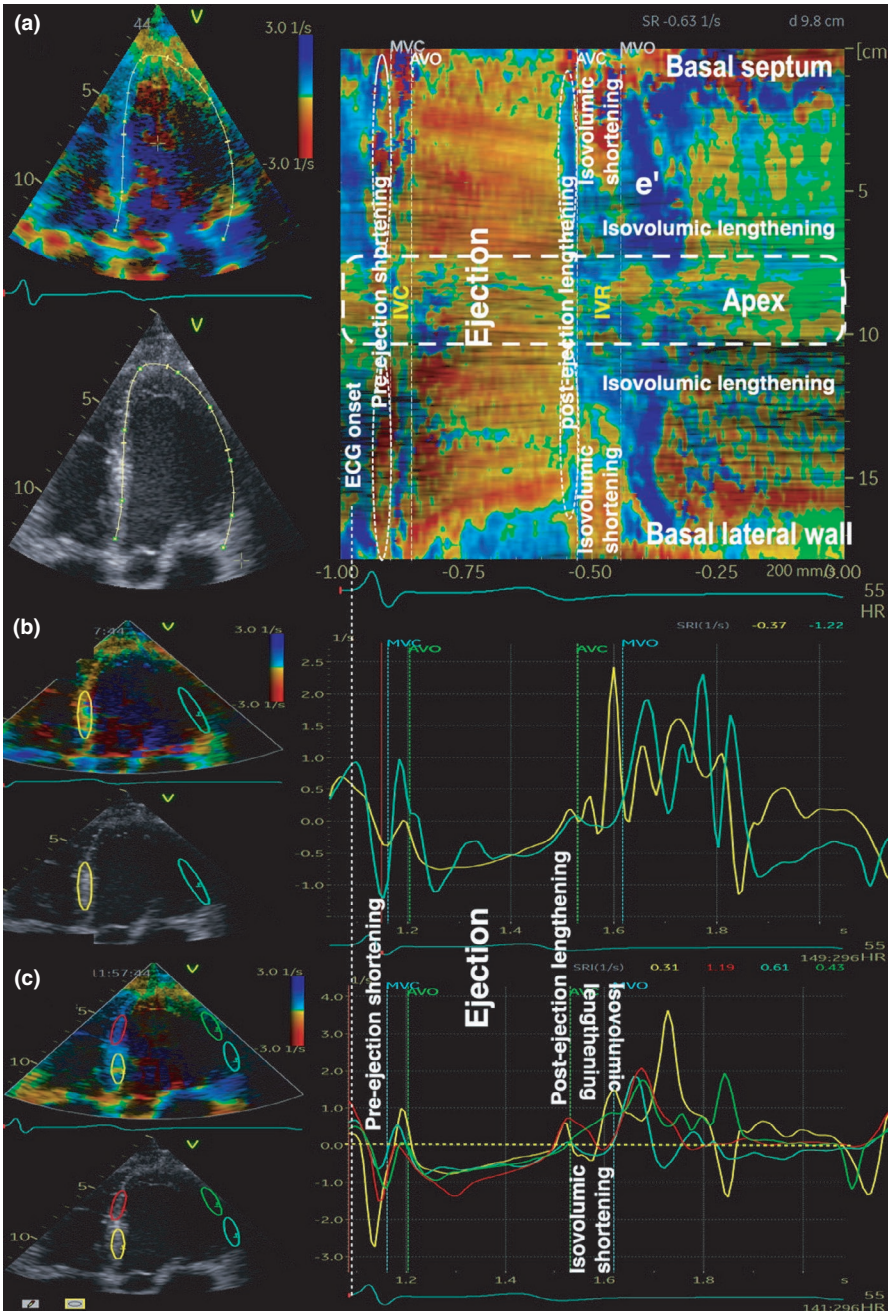

FIGURE 2 Strain rate imaging; colour M-mode and tracings from four-chamber view. (a) Colour CAMM from septal base through apex to lateral wall, (b) Full wall strain rate curves from septum and lateral wall, (c) Strain rate from the apical and basal parts of both walls separated. Longitudinal shortening (red colour, negative strain rate = is seen during pre-ejection and again during ejection, lengthening [blue colour/positive strain rate]) is seen in the post-ejection phase and early filling (e′). During IVR, the basal walls shorten, the apical walls lengthen

4.1 | Pre-ejection and MVC

The findings in this study are in accordance with a previous study with ultra-high frame rate TDI (Brekke, et al., 2014) showing that the pre-ejection spike occurs before MVC, and simultaneous in the two walls. Strain rate confirms this to be simultaneous shortening of the two walls. The pre-ejection spike represents the onset of active contraction, not recoil from atrial contraction, as it is present in atrial fibrillation, but absent in AV-block without subsequent ventricular activation (Brekke, et al., 2014). This being active contraction is also consistent with the pressure rise in the LV MVC (Dean, 1916; Laniado, et al., 1973; Tsakiris, et al., 1978; Wiggers, 1921), and especially with the simultaneous pressure increase and volume decrease of about 4.7% of EDV demonstrated by Remme et al., (2008). The simultaneity of the septum and lateral wall is consistent with the electrophysiological finding of simultaneous earliest breakthrough of electrical activation in the inferoseptal and anterolateral wall, 0–15 ms after initiation of QRS in surface ECG (Cassidy, et al., 1984) by the septal and posterior fascicles of the left bundle respectively. Electromechanical activation (onset of active shortening) is consistent with an electromechanical delay on the cellular level to onset of shortening of 20–30 ms (Cordeiro, et al., 2004) similar to the onset of pre-ejection velocities found by Brekke et al., (2014), and in the present study. In this pre-ejection phase, there is a small volume decrease before MVC, as demonstrated by Remme et al., (2008). This can also be seen by the small mitral annular displacement. As the apex is practically stationary, annulus displacement reflects LV length, which is proportional to LV volume (Støylen, et al., 2020).

TABLE 2 Time intervals by tissue Doppler

	Inferoseptal	Anterolateral
Velocity traces		
HR in TVI recordings (BPM)	65.8 (9.0)	
Q—onset pre-ejection spike (ms)	25.5 (7.8)	24.1 (12.4)
Duration of pre-ejection spike (ms)	51.0 (10.2)	52.0 (11.5)
Peak pre-ejection velocity (cm/s)	3.59 (1.56)	3.55 (1.58)
MVC—end pre-ejection spike (ms)	11.0 (12.9)	9.5 (9.4)[a]
AVO—rapid systolic velocity upstroke (ms)	3.8 (10.2)	1.0 (17.3)[a]
Duration protodiastolic spike (ms)	35.5 (10.7)	40.4 (11.2)
Peak protodiastolic velocity (cm/s)	−1.99 (1.38)	−1.78 (1.07)
AVC—end protodiastolic spike (ms)	9.5 (14.7)[a]	23.0 (15.5)[b]
Velocity CAMM		
Duration protodiastolic negative velocities (ms)	29.2 (8.6)	NA
AVC—end protodiastolic negative velocities (ms)	3.3 (6.2)	NA
Strain rate		
Peak pre-ejection strain rate (s^{-1})	−0.77 (0.61)	−0.66 (0.38)
Peak protodiastolic strain rate (s^{-1})	0.35 (0.31)	NA
Peak basal strain rate IVR (s^{-1})	−1.07 (0.74)	−0.36 (0.39)
Peak apical strain rate IVR (s^{-1})	0.36 (0.61)[c]	0.52 (0.65)[c]

Note: NA: not analysed in the lateral wall, due to low number.

Abbreviations: AVC, Aortic valve closure; AVO, Aortic valve opening; HR, Heart rate; IVR, Isovolumic relaxation time; MVC, Mitral valve closure.

[a]*p* for difference between spectral Doppler valve timing and TDI timing <0.001.

[b]*p* for difference between walls <0.001.

[c]*p* for difference between apex and base <0.001.

Displacement shows a small LV shortening at pre-ejection equivalent to the velocity spike, terminating with the MVC (Figure 3a,b), demonstrating a volume decrease, which is not due to flow, but to the relative motion of the mitral annulus in the stationary blood pool, excluding this volume before MVC (Figure 3d). The motion of the base in the blood pool will also force the mitral leaflets backwards towards coaptation (Figure 3d) by the resistance of the blood, possibly in combination with the intraventricular vortex after the A-wave (Hong, et al., 2008). MVC itself, by the suddenly increased resistance, will cause an abrupt termination of this motion of the LV base. Remme demonstrated this elegantly by stenting of the mitral valve; causing the pre-ejection velocity to continue directly into the ejection phase (Remme, et al., 2008). The IVC by Doppler in this study corresponded roughly to the IVC by tissue Doppler when pre-ejection velocity was excluded, and with previous findings (Hirschfeld, et al., 1976). Including the pre-ejection spike, will overestimate IVC by about 40 ms. Colour M-mode of the mitral valve will correctly identify MVC by the end of downward leaflet motion, which means the pre-ejection spike will not be visible. Thus, active contraction starts with a small volume and length decrease before MVC, followed by IVC, which, of course ends with aortic valve opening (AVC). The main myocardial deformation is seen by volume and length decrease occurs during the ejection phase, but this marks the AVC, not the electromechanical activation, as has been maintained by Andersen et al., (2019).

4.2 | Post-ejection and AVC

At end ejection, there is a short event of negative velocity seen as a negative spike by velocity traces, and blue colour of negative velocity in CAMM, both in the septum and the mitral leaflet (Figure 1). Duration of the velocity spike was similar between the walls, but with a delay in the lateral wall, which may be some error in timing here, due to the predominant negative velocities in the lateral wall. Duration of the event was less by colour TDI but the end corresponded more closely to the AVC. Elongation after ejection could also be seen by SRI (Figure 2), also in strain rate predominantly in the septum. We have previously shown both by phonocardiography and HFR TDI that AVC occurred at the end of this event (Aase, et al., 2006; Aase, et al., 2008; Slørdahl, et al., 2001). Physiologically, relaxation, which primarily is tension devolution, starts at peak LV pressure; the last part of ejection being driven by pressure and inertial flow. But with continuing ejection, there will still be volume decrease and wall shortening until end ejection. At end ejection, flow will be zero. Further myocardial relaxation will result in wall elongation. This is seen as a slight downwards motion in the septum (Figure 3c), ending abruptly at AVC in a 'notch'. This lengthening is equivalent to the negative velocity spike (Figure 3b) and positive strain (Figure 2). During this phase, the displacement of the aortic annulus will result in a slight volume increase, to be 1.6% of EDV (Remme, et al., 2008), ending at the dicrotic notch, thus being pre-AVC. The volume increase is not due to flow, but to the aortic annulus moving in a stationary blood column, engulfing the volume before AVC (Figure 3). As the mitral valve is closed during this phase, the mitral annulus will offer a considerable resistance to LV lengthening in the lateral part, consistent with the observed asymmetry in motion. The volume increase after the end of flow explains the increase in the rate of pressure drop seen just before the dicrotic notch (Spencer & Greiss, 1962; Wiggers, 1921), and thus, the post-ejection phase is the protodiastole (Wiggers, 1921). Motion of the aortic annulus away from the apex in a stationary blood column will in itself force the aortic cusps towards closure as illustrated in Figure 3. The post-ejection

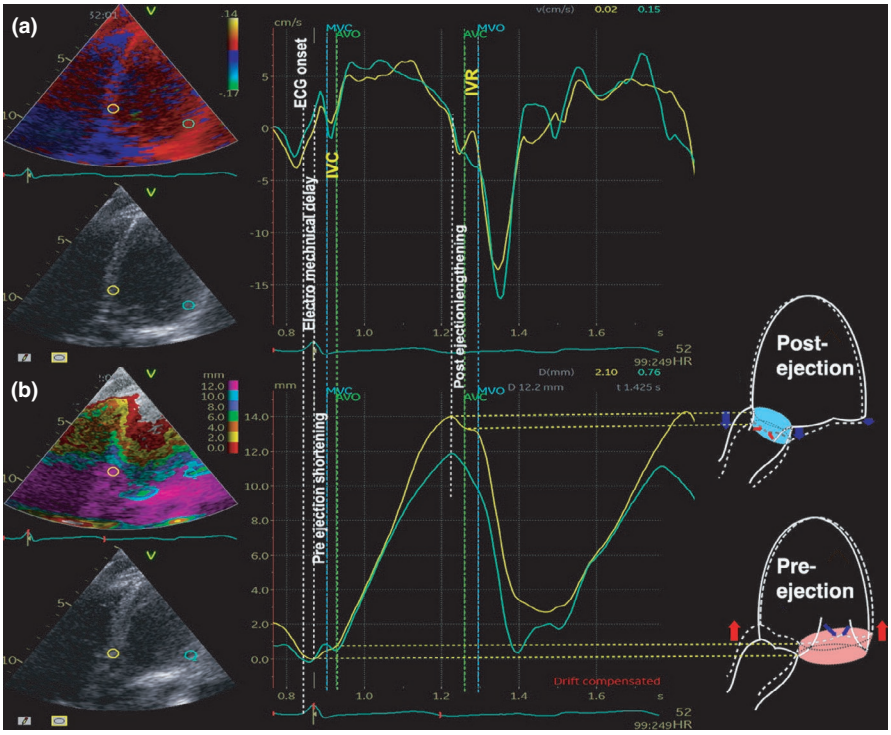

FIGURE 3 Relation of AV-plane motion and LV volume changes. (a) Velocity traces and (b) displacement traces, showing that the pre- and post-ejection velocity traces correspond to small length changes of the left ventricle, which again results in small volume changes at the open orifices moves in nearly stationary blood. Pre-ejection shortening before mitral valve closure excludes a small volume (light red), as shown in the diagram to the left, post-ejection lengthening before aortic valve closure engulfs a small volume (light blue)

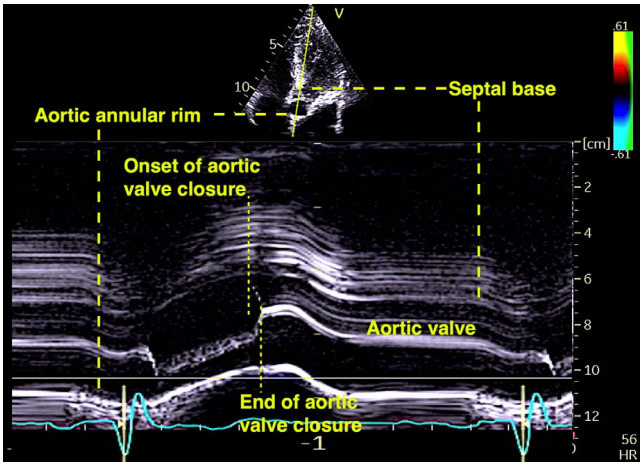

FIGURE 4 Skewed M-mode through septum, aortic valve and posterior aortic annular rim. The M-mode shows the closure of the aortic valve to be an event with a certain duration, ending with the full closure, in this recording, there is an indication that this is simultaneous with the 'notch' at the end of post-ejection lengthening

lengthening is thus part of the mechanism for AVC, and the final closure of the valve the cause of the termination of the post-ejection lengthening. Remme showed this by stenting of the aortic valve, which caused the post-ejection negative velocity to continue directly into the negative velocities of early filling (Remme, et al., 2008). Thus, vortex formation behind the cusps does not seem to be the main mechanism, but in the presence of sinuses, vortices would form behind the leaflets, persisting after peak flow and starting to force the cusps away from the wall before end systole (Bellhouse & Bellhouse, 1968). This mechanism will, of course, increase the tendency for the cusps to close due to annular motion. As the AVC is the end of the post-ejection lengthening, this means protodiastole is the period of aortic valve closure from fully open to fully close as illustrated in Figure 4.

Including the post-ejection velocities in the IVR will shorten the ejection time by about 38 ms if velocity traces are used, 29 ms if septal colour Doppler is used and prolong IVR by a similar amount. In addition, the feasibility of CAMM for identifying the end of pre-ejection lengthening is low. Using the mitral valve colour M-mode, Kjaergaard et al., (2005) identified the onset of lengthening but taking that as AVC gives an error of about 24 ms while it has a low feasibility for the end of lengthening. However, using the onset as surrogate, the feasibility is better, and the real difference is small.

4.3 | Isovolumic relaxation

True IVR shows lengthening in the apex and shortening in the base by strain rate (Figure 2). The elongation is probably related to the 'untwisting' of the apex (Rademakers, et al., 1992; Takeuchi, et al., 2006). This shows IVR to be a quite dynamic phase, not only pressure relaxation. Negative strain rate does not necessarily indicate that the shortening in the base is active contraction, but that it may be a reciprocal effect of the apical lengthening, as the volume is constant. But the opposing deformations will cause a volume shift from the base to the apex and explain both the intraventricular flow (Sasson, et al., 1987) and the pressure gradient towards the apex (Nikolic, et al., 1995) in IVR. The initiation of flow towards apex during IVR thus initiates a momentum before start of early filling. Thus, the basal shortening during IVR is physiological, despite paired with simultaneous apical elongation, and regarding this as wasted work (Manganaro et al., 2020), is physiologically erroneous.

4.4 | Limitations

This study has used conventional colour TDI. With a frame rate of 133, this means 7.5 ms per frame, and in the analysis software, the minimum time measurement was 10 ms.

As pre-ejection and protodiastolic velocities are short-lived events, this means that there is a risk of undersampling that will affect both peak values and variability (Lind, et al., 2002). Thus, peak values have a low reliability. It also means that there is a tendency to drift in the velocity data, so not only peaks but also nadirs of the spikes will vary somewhat. In addition, the exact end of the velocity spikes is unclear. Using the nadir after the spike is an approximation at best, as seen in Figure 1c. By UHFR-TDI, the pre-ejection motion can be resolved into greater detail, which could delineate the start and end of the events in more detail (Brekke, et al., 2014). Secondly, colour imaging and traces are not completely equivalent, despite the underlying data being the same. Timing in colour images is shown by red–blue transitions, which are located where the velocity traces cross zero. This can be seen in Figure 1d. The zero values are the shift in displacement directions and thus should be closest to valve closures (Aase, et al., 2008). Thus, CAMM is more precise as valve closure markers, but with a lower feasibility.

Time intervals are HR dependent (Stoylen, et al., 2003), and the valve movements and tissue Doppler data are from different heart cycles. In the present study, the difference was small, although significant.

Strain rate has an unfavourable noise-to-signal ratio, resulting in even more variability of peak values, and the clutter noise also renders exact timing in colour strain rate less feasible. The advantage of strain rate is the ability to differentiate shortening and lengthening along each wall, while tethering renders velocities unfeasible for this.

5 | CONCLUSIONS

The present study shows electromechanical LV activation occurring simultaneously in both the septum and the lateral wall, before MVC, visible as pre-ejection velocity spikes in conventional tissue Doppler. This early contraction contributes to MVC. These velocities are not a part of IVC. LV relaxation is a continuous process from peak pressure though IVR and the e′ wave. Lengthening starts at end ejection where flow is zero, and the motion of the aortic annulus in the blood column contributes to the AVC itself. The post-ejection phase is the period of aortic valve closure. Pre- and post-ejection tissue velocity spikes should not be included in the isovolumic phases. The clinical interest is basically that the data correct how the Tei index should be derived from tissue Doppler data.

Isovolumetric relaxation is characterized by apical elongation and basal shortening, which will result in a volume shift from base to apex, being constructive work initiating apical flow before early filling and should not be designed as wasted work.

ACKNOWLEDGEMENTS

The study was in part financed by a grant from the mid-Norwegian regional health authorities.

CONFLICT OF INTEREST

None.

DATA AVAILABILITY STATEMENT

Data will be available at reasonable request.

ORCID

Asbjørn Støylen https://orcid.org/0000-0002-2245-7066

REFERENCES

Aase, S.A., Stoylen, A., Ingul, C.B., Frigstad, S. & Torp, H. (2006) Automatic timing of aortic valve closure in apical tissue Doppler images. *Ultrasound in Medicine & Biology*, *32*, 19–27.

Aase, S.A., Torp, H. & Støylen, A. (2008) Aortic valve closure: relation to tissue velocities by Doppler and speckle tracking in normal subjects. *European Journal of Echocardiography: The Journal of the Working Group on Echocardiography of the European Society of Cardiology*, *9*, 555–559.

Andersen, M.V., Moore, C., Søgaard, P., Friedman, D., Atwater, B.D., Arges, K. et al. (2019) Quantitative parameters of high-frame-rate strain in patients with echocardiographically normal function. *Ultrasound in Medicine & Biology*, *45*, 1197–1207.

Bellhouse, B.J. & Bellhouse, F.H. (1968) Mechanism of closure of the aortic valve. *Nature*, *217*, 86–87.

Brekke, B., Nilsen, L.C., Lund, J., Torp, H., Bjastad, T., Amundsen, B.H. et al. (2014) Ultra-high frame rate tissue Doppler imaging. *Ultrasound in Medicine & Biology*, *40*, 222–231.

Cassidy, D.M., Vassallo, J.A., Marchlinski, F.E., Buxton, A.E., Untereker, W.J. & Josephson, M.E. (1984) Endocardial mapping in humans in sinus rhythm with normal left ventricles: activation patterns and characteristics of electrograms. *Circulation*, *70*, 37–42.

Cordeiro, J.M., Greene, L., Heilmann, C., Antzelevitch, D. & Antzelevitch, C. (2004) Transmural heterogeneity of calcium activity and mechanical function in the canine left ventricle. *American Journal of Physiology Heart and Circulatory Physiology*, *286*, H1471–H1479.

Dean, A.L. (1916) The movements of the mitral cusps in relation to the cardiac cycle. *American Journal of Physiology-Legacy Content*, *40*(2), 206–217, Washington.

Derumeaux, G., Ovize, M., Loufoua, J., André-Fouet, X., Minaire, Y., Cribier, A. et al. (1998) Doppler tissue imaging quantitates regional wall motion during myocardial ischemia and reperfusion. *Circulation*, *97*, 1970–1977.

Edvardsen, T., Urheim, S., Skulstad, H., Steine, K., Ihlen, H. & Smiseth, O.A. (2002) Quantification of left ventricular systolic function by tissue Doppler echocardiography: added value of measuring pre- and postejection velocities in ischemic myocardium. *Circulation*, *105*, 2071–2077.

Hatle, L. (1981) Noninvasive assessment and differentiation of left ventricular outflow obstruction with Doppler ultrasound. *Circulation*, *64*, 381–387.

Hirschfeld, S., Liebman, J., Borkat, G. & Bormuth, C. (1977) Intracardiac pressure-sound correlates of echographic aortic valve closure. *Circulation*, *55*, 602–604.

Hirschfeld, S., Meyer, R., Korfhagen, J., Kaplan, S. & Liebman, J. (1976) The isovolumic contraction time of the left ventricle. An echographic study. *Circulation*, *54*, 751–756.

Hong, G.R., Pedrizzetti, G., Tonti, G., Li, P., Wei, Z., Kim, J.K. et al. (2008) Characterization and quantification of vortex flow in the human left

ventricle by contrast echocardiography using vector particle image velocimetry. *JACC Cardiovascular Imaging*, *1*, 705–717.

Kjaergaard, J., Hassager, C., Oh, J.K., Kristensen, J.H., Berning, J. & Sogaard, P. (2005) Measurement of cardiac time intervals by Doppler tissue M-mode imaging of the anterior mitral leaflet. *Journal of the American Society of Echocardiography: Official Publication of the American Society of Echocardiography*, *18*, 1058–1065.

Laniado, S., Yellin, E.L., Miller, H. & Frater, R.W. (1973) Temporal relation of the first heart sound to closure of the mitral valve. *Circulation*, *47*, 1006–1014.

Lind, B., Eriksson, M., Roumina, S., Nowak, J. & Brodin, L.A. (2006) Longitudinal isovolumic displacement of the left ventricular myocardium assessed by tissue velocity echocardiography in healthy individuals. *Journal of the American Society of Echocardiography: Official Publication of the American Society of Echocardiography*, *19*, 255–265.

Lind, B., Nowak, J., Dorph, J., van der Linden, J. & Brodin, L.A. (2002) Analysis of temporal requirements for myocardial tissue velocity imaging. *European Journal of Echocardiography: The Journal of the Working Group on Echocardiography of the European Society of Cardiology*, *3*, 214–219.

Lyseggen, E., Rabben, S.I., Skulstad, H., Urheim, S., Risoe, C. & Smiseth, O.A. (2005) Myocardial acceleration during isovolumic contraction: relationship to contractility. *Circulation*, *111*, 1362–1369.

Manganaro, R., Marchetta, S., Dulgheru, R., Sugimoto, T., Tsugu, T., Ilardi, F. et al. (2020) Correlation between non-invasive myocardial work indices and main parameters of systolic and diastolic function: results from the EACVI NORRE study. *European heart journal cardiovascular Imaging*, *21*, 533–541.

Nikolic, S.D., Feneley, M.P., Pajaro, O.E., Rankin, J.S. & Yellin, E.L. (1995) Origin of regional pressure gradients in the left ventricle during early diastole. *American Journal of Physiology*, *268*, H550–557.

Rademakers, F.E., Buchalter, M.B., Rogers, W.J., Zerhouni, E.A., Weisfeldt, M.L., Weiss, J.L. et al. (1992) Dissociation between left ventricular untwisting and filling. Accentuation by catecholamines. *Circulation*, *85*, 1572–1581.

Remme, E.W., Lyseggen, E., Helle-Valle, T., Opdahl, A., Pettersen, E., Vartdal, T. et al. (2008) Mechanisms of preejection and postejection velocity spikes in left ventricular myocardium: interaction between wall deformation and valve events. *Circulation*, *118*, 373–380.

Sasson, Z., Hatle, L., Appleton, C.P., Jewett, M., Alderman, E.L. & Popp, R.L. (1987) Intraventricular flow during isovolumic relaxation: description and characterization by Doppler echocardiography. *Journal of the American College of Cardiology*, *10*, 539–546.

Slørdahl, S.A., Bjaerum, S., Amundsen, B.H., Støylen, A., Heimdal, A., Rabben, S.I. et al. (2001) High frame rate strain rate imaging of the interventricular septum in healthy subjects. *European Journal of Ultrasound: Official Journal of the European Federation of Societies for Ultrasound in Medicine and Biology*, *14*, 149–155.

Spencer, M.P. & Greiss, F.C. (1962) Dynamics of ventricular ejection. *Circulation research*, *10*, 274–279.

Støylen, A., Dalen, H. & Molmen, H.E. (2020) Left ventricular longitudinal shortening: relation to stroke volume and ejection fraction in ageing, blood pressure, body size and gender in the HUNT3 study. *Open Heart*, *7*(2), e001243.

Stoylen, A., Wisløff, U. & Slørdahl, S. (2003) Left ventricular mechanics during exercise: a Doppler and tissue Doppler study. *European Journal of Echocardiography: The Journal of the Working Group on Echocardiography of the European Society of Cardiology*, *4*, 286–291.

Takeuchi, M., Nakai, H., Kokumai, M., Nishikage, T., Otani, S. & Lang, R.M. (2006) Age-related changes in left ventricular twist assessed by two-dimensional speckle-tracking imaging. *Journal of the American Society of Echocardiography: Official Publication of the American Society of Echocardiography*, *19*, 1077–1084.

Tsakiris, A.G., Gordon, D.A., Padiyar, R. & Fréchette, D. (1978) Relation of mitral valve opening and closure to left atrial and ventricular pressures in the intact dog. *American Journal of Physiology*, *234*, H146–151.

Van de Veire, N.R., De Sutter, J., Bax, J.J. & Roelandt, J.R. (2008) Technological advances in tissue Doppler imaging echocardiography. *Heart (British Cardiac Society)*, *94*, 1065–1074.

Vogel, M., Schmidt, M.R., Kristiansen, S.B., Cheung, M., White, P.A., Sorensen, K. et al. (2002) Validation of myocardial acceleration during isovolumic contraction as a novel noninvasive index of right ventricular contractility: comparison with ventricular pressure-volume relations in an animal model. *Circulation*, *105*, 1693–1699.

Voigt, J.U., Lindenmeier, G., Exner, B., Regenfus, M., Werner, D., Reulbach, U. et al. (2003) Incidence and characteristics of segmental postsystolic longitudinal shortening in normal, acutely ischemic, and scarred myocardium. *Journal of the American Society of Echocardiography: Official Publication of the American Society of Echocardiography*, *16*, 415–423.

Wiggers, C.J. (1921) Studies on the consecutive phases of the cardiac cycle. *American Journal of Physiology-Legacy Content*, *56*, 415–438.

How to cite this article: Støylen, A., & Daae, A. S. (2021). Physiological significance of pre- and post-ejection left ventricular tissue velocities and relations to mitral and aortic valve closures. *Clinical Physiology and Functional Imaging*, 41, 443–451. https://doi.org/10.1111/cpf.12721